*Clinical Science* (2024) **138** 851–862
https://doi.org/10.1042/CS20240346

PORTLAND PRESS

Research Article

# The endothelin-1-driven tumor-stroma feed-forward loops in high-grade serous ovarian cancer

**Piera Tocci[1], Celia Roman[1], Rosanna Sestito[1], Valentina Caprara[1], Andrea Sacconi[2], Ivan Molineris[3], Giovanni Tonon[4,5], Giovanni Blandino[2] and Anna Bagnato[1]**

[1]Preclinical Models and New Therapeutic Agents Unit, Istituto di Ricovero e Cura a Carattere Scientifico (IRCCS), Regina Elena National Cancer Institute, Rome, Italy; [2]Translational Oncology Research Unit, IRCCS, Regina Elena National Cancer Institute, Rome, Italy; [3]Department of Life Science and System Biology, University of Turin, Turin, Italy; [4]Center for Omics Sciences (COSR) and Functional Genomics of Cancer Unit, Division of Experimental Oncology, IRCCS San Raffaele Scientific Institute, Milan, Italy; [5]Università Vita-Salute San Raffaele, 20132, Milan, Italy

**Correspondence:** Anna Bagnato (annateresa.bagnato@ifo.it) or Piera Tocci (piera.tocci@ifo.it)



The high-grade serous ovarian cancer (HG-SOC) tumor microenvironment (TME) is constellated by cellular elements and a network of soluble constituents that contribute to tumor progression. In the multitude of the secreted molecules, the endothelin-1 (ET-1) has emerged to be implicated in the tumor/TME interplay; however, the molecular mechanisms induced by the ET-1-driven feed-forward loops (FFL) and associated with the HG-SOC metastatic potential need to be further investigated. The tracking of the patient-derived (PD) HG-SOC cell transcriptome by RNA-seq identified the vascular endothelial growth factor (VEGF) gene and its associated signature among those mostly up-regulated by ET-1 and down-modulated by the dual ET-1R antagonist macitentan. Within the ligand–receptor pairs concurrently expressed in PD-HG-SOC cells, endothelial cells and activated fibroblasts, we discovered two intertwined FFL, the ET-1/ET-1R and VEGF/VEGF receptors, concurrently activated by ET-1 and shutting-down by macitentan, or by the anti-VEGF antibody bevacizumab. In parallel, we observed that ET-1 fine-tuned the tumoral and stromal secretome toward a pro-invasive pattern. Into the fray of the HG-SOC/TME double and triple co-cultures, the secretion of ET-1 and VEGF, that share a common co-regulation, was inhibited upon the administration of macitentan. Functionally, macitentan, mimicking the effect of bevacizumab, interfered with the HG-SOC/TME FFL-driven communication that fuels the HG-SOC invasive behavior. The identification of ET-1 and VEGF FFL as tumor and TME actionable vulnerabilities, reveals how ET-1R blockade, targeting the HG-SOC cells and the TME simultaneously, may represent an effective therapeutic option for HG-SOC patients.

## Introduction

The tumor microenvironment (TME) represents the habitat in which tumor cells live and expand in communion with a myriad of elements, including the extracellular matrix (ECM), and multiple types of stromal elements [1–3]. In the high-grade serous ovarian cancer (HG-SOC), the most frequent and severe form of ovarian cancer frequently diagnosed in later stages [1], the dynamic co-evolution of tumor cells with the surrounding TME, corrupting homeostatic networks, impacts on its invasive and metastatic journey [4–6].

In the tumor/TME interplay a complex system of bioactive circulating molecules, including cytokines, chemokines, growth factors and inflammatory mediators, is at the heart of the intercellular communication [2,6]. In particular, tumor cells secrete biological factors to educate the neighboring TME cells for their own growth and dissemination benefits. On their part, TME elements release signals that facilitate the metastatic odyssey. Such reciprocal tumor/TME cross-talk provides to cancer cells a therapy elusive attitude, contributing to disease progression [2,4,7–9]. Remarkably, it was observed how the high

Received: 23 February 2024
Revised: 30 May 2024
Accepted: 17 June 2024

Accepted Manuscript online: 17 June 2024
Version of Record published: 05 July 2024

*Clinical Science* (2024) **138** 851–862
https://doi.org/10.1042/CS20240346

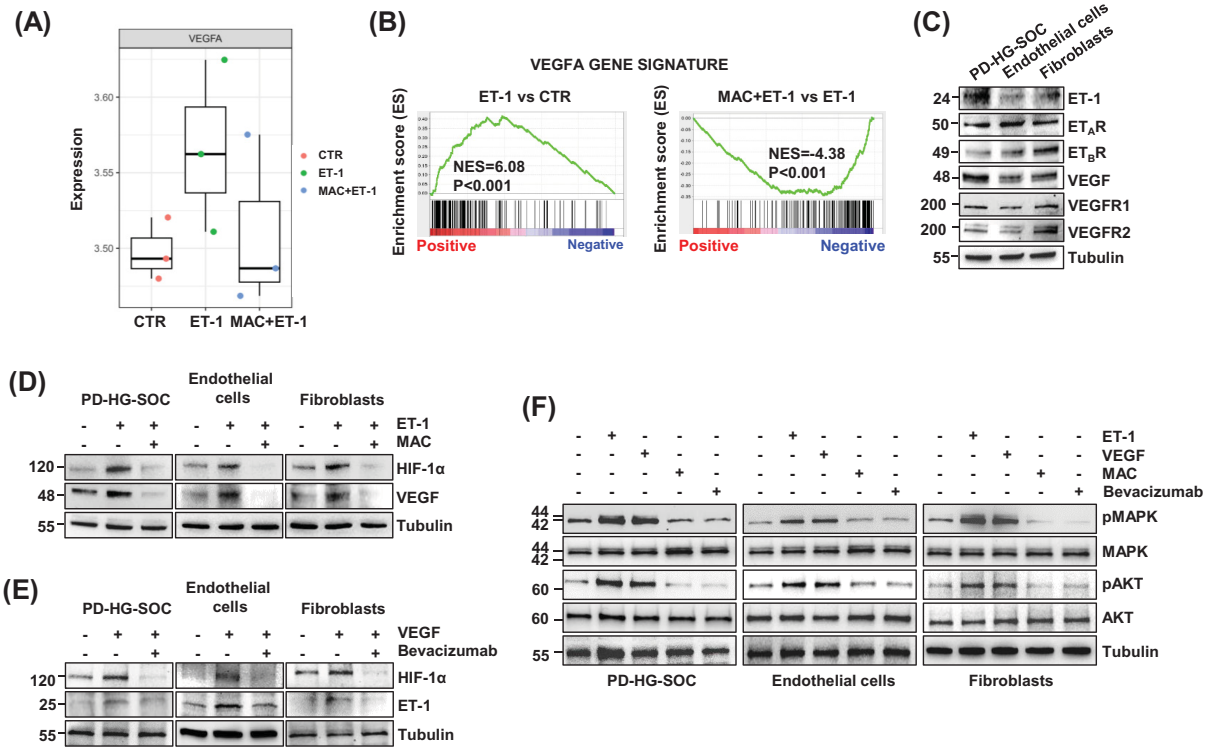


**Figure 1. The ET-1/ET-1R FFL intertwines with the VEGF/VEGFR axis and sustains pro-survival pathways in HG-SOC cells and stromal elements**

(**A**) Box-plot of *VEGFA* levels (expressed in reads for kilobase million) in RNAseq-analyzed PD-HG-SOC cells stimulated or not with ET-1 (100 nM) or treated with macitentan (MAC, 1 μm) plus ET-1 for 24 h. (**B**) ET-1 enriches the VEGFA associated gene signature in PD-HG-SOC cells. GSEA in cells stimulated with ET-1 or treated with MAC plus ET-1 for 24 h with the normalized enrichment score (NES). (**C**) Immunoblotting (IB) analysis for ET-1, $ET_AR$, $ET_BR$, VEGF, VEGFR1, VEGFR2, in total extracts of patient-derived (PD) HG-SOC cells, endothelial cells (EC) and activated fibroblasts. Tubulin was used as a loading control. (**D,E**) IB analysis for HIF-1α and VEGF (D) or HIF-1α and ET-1 (E) in total extracts of PD-HG-SOC cells, EC and activated fibroblasts stimulated with ET-1 or treated with MAC for 24 h (D) or stimulated with VEGF and treated with bevacizumab for 24 h (E). Tubulin was used as a loading control. (**F**). IB analysis for pMAPK, MAPK, pAKT and AKT in total extracts of PD-HG-SOC cells, EC and activated fibroblasts stimulated with ET-1 or VEGF (50 ng/ml) for 30 min or treated for 30 min with macitentan or bevacizumab (250 μg/ml). Tubulin was used as a loading control.

abundance of stromal cells in the HG-SOC TME is significantly associated with a shortened life expectancy [6,10] and the poor response to chemotherapy [11,12].

A major class of secreted mediators implicated in the cell–cell communication comprises growth factors that activate their cognate receptors expressed by both tumor and TME cells. Within this unique subset of circulating ligands, the endothelin-1 (ET-1) and the vascular endothelial growth factor (VEGF), binding the ET-1 receptors (ET-1R) A and B ($ET_AR$ and $ET_BR$) and the VEGF receptor 1 and 2 (VEGFR1 and VEGFR2), respectively, have been described to unleash, through both autocrine and paracrine signaling routes, tumor growth, metastatization, new blood vessel formation and poor response to the available therapeutics for HG-SOC [13–18]. Remarkably, high levels of ET-1 were detected in the ascitic fluids of ovarian cancer patients and correlated with VEGF levels [19]. In this tumor, ET-1/$ET_AR$ axis induced VEGF expression through the hypoxia-inducible factor (HIF-1α) [20]. In this respect, it was recently demonstrated that the ET-1R-driven HIF-1α transcriptional machinery, rewiring the tumor and TME behavior, regulates the DNA damage response and contributes to the HG-SOC poor response to the PARP inhibitor olaparib [16]. Despite these observations, gaining a more comprehensive view of the ET-1-driven mechanisms at the core of the tumor/TME communication, particularly those related to the instigation of self-enhancing signaling loops able to enforce the tumor metastatic nature, can be used as a tactic to interrupt this interplay, implementing the antimetastatic therapeutic strategies in HG-SOC.

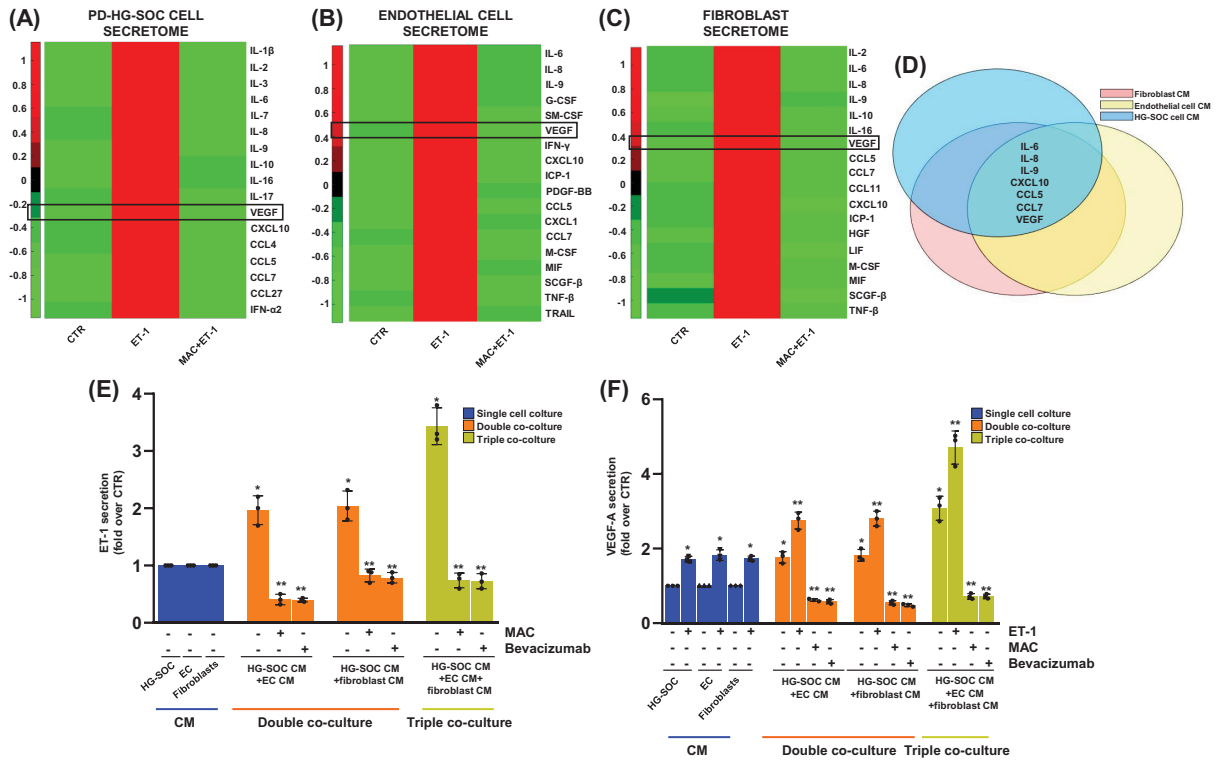


**Figure 2. The ET-1/ET-1R FFL fine-tunes the tumoral and stromal cell secretome**

(**A–C**) Heatmap of the mean standardized fluorescence intensity of cytokines and chemokines in PD-HG-SOC, endothelial cells (EC) and activated fibroblasts conditioned media (CM) stimulated or not with ET-1 for 24 h or treated with MAC+ET-1 for 24 h. Factors were clustered based on Euclidean distance. Cytokine and chemokine expression, evaluated under different conditions, were standardized by rows and represented as a heatmap, with a color scale from green (lower levels) to red (higher levels). The heatmaps were generated using the Matlab R2023b program. (**D**). Venn diagram indicating the factors communally released by PD-HGSOC cells (light blue), EC (yellow) and activated fibroblasts (pink). (**E,F**) ELISA for ET-1 (E) and VEGF (F) released by PD-HG-SOC cells, EC and activated fibroblasts in single cell culture, or in PD-HG-SOC/EC or PD-HG-SOC/activated fibroblasts double cell culture, or PD-HG-SOC/EC/activated fibroblasts triple cell culture, stimulated or not with ET-1 for 24 h or treated with MAC or bevacizumab for 24 h. Bars are means ± SD (E: *$P$<0.003 vs. untreated single cell culture; **$P$<0.002 vs. untreated double or triple co-culture; $n$=3. F: *$P$<0.003 vs. ET-1 untreated single cell culture; **$P$<0.004 vs. ET-1 or MAC or bevacizumab untreated double or triple cell co-culture; $n$=3).

Considering the inadequacy of the available therapeutics for HG-SOC, in the present study, we aimed to elucidate how specific ligand–receptor interactions, as the ET-1/ET-1R and VEGF/VEGFR axes, activating self-sustaining signaling flows at the HG-SOC/TME interface, may prime the establishment of a tumor permissive TME. Additionally, we evaluated how the targeting of the ET-1/ET-1R FFL, simultaneously hitting the VEGF/VEGFR FFL in the tumor and in the TME, may embody a successful therapeutic strategy for HG-SOC patients.

# Materials and methods

## Cell lines and chemical compounds

Patient-derived (PD) HG-SOC cells were isolated from the ascitic fluid of a HG-SOC patient undergoing surgery for ovarian tumor by laparotomy or paracentesis at the Gynaecological Oncology of our Institute. This cell line is named PMOV10 where PM stands for Preclinical Models, OV stands for ovarian serous cancer, and # is the order in which the cell line was established. PMOV10 (*TP53* mutant R337T) closely recapitulates the genomic traits, the histopathology and the molecular features of the HG-SOC patient (stage III, age 69) [14]. The ascitic sample collection together with the relative clinical information were approved by the Regina Elena institutional review board (IRB) after HG-SOC patients gave written informed consent. Briefly, cells were harvested by centrifugation at 200 × ***g*** for 5 min at room temperature, resuspended in Dulbecco's PBS, and then centrifuged through Ficoll-Histopaque

*Clinical Science* (2024) **138** 851–862
https://doi.org/10.1042/CS20240346

1077 (Sigma-Aldrich, St. Louis, Missouri, U.S.A.). Interface cells were washed in culture medium, and $5 \times 10^6$ viable cells were seeded in 75-$cm^2$ culture flasks, in RPMI 1640 (Gibco, Grovemont Cir, Gaithersburg, U.S.A.) containing 1% penicillin-streptomycin and 10% fetal bovine serum. The purity of primary cultures was assessed by immunophenotyping with a panel of monoclonal Abs (including WT1, keratin 7, calretinin and OCT-125) recognizing ovarian tumor-associated antigens by the alkaline phosphatase-peroxidase-antiperoxidase method.

Human lung fibroblasts (WI-38, CCL-75 ATCC) and Human Umbilical Vein Endothelial Cells (HUVEC; Lonza) were maintained as indicated [16]. Cell lines were authenticated by STR profiling and regularly controlled for mycoplasma infection. ET-1 (Sigma-Aldrich, MO, U.S.A.) was used at a 100 nM final concentration. Macitentan (Selleckchem, United Kingdom), also called ACT-064992 or N-[5-(4-Bromophenyl)-6-[2-[(5-bromo-2-pyrimidinyl)oxy]ethoxy]-4-pyrimidinyl]-N′-propyl-sulfamide, added 30 min before ET-1 when administered in combination, was used at a 1 μM final concentration. VEGFA was used at 50 ng/ml (R&D Systems, Minneapolis, MN). Bevacizumab, also known as MVASI, was used at a 250 μg/ml final concentration.

## Immunoblotting (IB)

Whole-cell lysates were obtained as reported [14] and were used for electrophoresis on SDS-PAGE gels. Bands with the protein of interest were detected by using the enhanced chemiluminescence (ECL) detection from Bio-Rad (CA, U.S.A.). The antibodies used for the study were as follows: Anti-ET-1 (cat. #ab88093, 1:1000) was from Abcam (cambridge, United United Kingdom). Anti-$ET_AR$ (cat. #PA3-065, 1:3000) was from Thermo Fisher Scientific (MA, U.S.A.). Anti-$ET_BR$ (cat. #sc-33538, 1:200), anti-VEGF (cat. #sc-53462, 1:200), anti-VEGFR1 (cat. #sc-316, 1:200), anti-VEGFR2 (cat. #sc-504, 1:200) and anti-Tubulin (cat. #sc-32293, 1:200) were from Santa Cruz Biotechnology (CA, U.S.A.). Anti-p-p44/42 MAPK (Thr202/Tyr204) (cat. #4377S, 1:1000), anti-p44/42 MAPK (cat. #9102, 1:1000) anti-pAkt (S473) (cat. #9271S, 1:1000) and anti-Akt (cat. #9272S, 1:1000) were from Cell Signaling Technology (MA, USA).

## Cytokine and chemokine analysis

PD-HG-SOC cells, HUVEC and WI-38 fibroblasts plated in 100 mm dish were serum-starved for 24 h and then stimulated or not with ET-1 and/or treated with macitentan for 48 h. Conditioned media (CM) were first collected and centrifuged at 1000 rpm in order to eliminate debris and second; they were used for the Luminex assay, where coupled magnetic beads and premixed detection antibodies are used for the quantification of the relevant targets. The different CM were profiled for cytokines and chemokines using a Bio-Plex Pro Human Cytokine Screening 48-Plex panel (Bio-Rad) according to the manufacturer's instructions. The cytokine/chemokine contents of each well were identified and quantified using a Bio-Plex Magpix apparatus (Bio-Rad) by comparing them to standard samples. The Matlab R2023b program was used to generate the heatmaps.

## ELISA assay

CM derived from PD-HG-SOC cells, HUVEC and WI-38 fibroblasts or from PD-HG-SOC, HUVEC and WI-30 double or triple direct co-culture (ratio 1:1 or 1:1:1) serum-starved for 24 h and then stimulated or not with exogenous ET-1 or treated with macitentan or bevacizumab for 48 h, were analysed for the release of ET-1 and VEGF by using Quantikine ELISA kits for human Endothelin-1 or human VEGF (R&D Systems, MN, U.S.A.) according to manufacturer's instructions.

## RNA sequencing of patient-derived HG-SOC cells

Total RNA from PD-HG-SOC cells was isolated by using the RNeasy Quick Start kit (Qiagen, Germany) according to manufacturer's instructions. NanoDrop (Thermo Scientific) was used to check RNA concentration, quality and purity. Before starting with library preparation, the quality of the RNA was set by running samples on the 4100 TapeStation system (Agilent, CA, U.S.A.). To generate the NGS libraries, we used the TruSeq Stranded mRNA kit (Illumina, CA, U.S.A.), starting with 100 ng of total RNA. Only RNA samples with RNA Integrity Number (RIN) above 7 were used in the next steps. Libraries were barcoded, pooled, and sequenced on an Illumina 6 NextSeq 500 sequencing system to obtain ∼20–30 million (M) single-end reads, 100 nt long, for each sample. Sequencing reads were aligned to the human reference genome GRCm38 using STAR v2.5.3a [21] (with parameters –outFilterMismatchNmax 999 –outFilterMismatchNoverLmax 0.04) and a list of known splice sites extracted from GENCODE 24 comprehensive annotation. Gene expression levels were quantified with featureCounts v1.6.3 [22] (options: -t exon -g gene_name) using GENCODE 24 basic gene annotation. Following gene expression counts were analyzed using the edgeR package

[23]. Normalization factors were performed using the trimmed-mean of M-values (TMM) method (implemented in the calcNormFactors function), and normalized library sizes and gene lengths were used to obtain Reads Per Kilobase Million (RPKM). Upon filtering low-ranking expressed genes (below 1 Counts Per Million [CPM] in 4 or more samples), differential expression analysis was conducted by fitting a Generalized Linear Model (GLM) to all groups, performing a Likelihood F (LF) test for the interesting pairwise contrasts. Genes were considered significantly differentially expressed when $|\log FC| > 1$ and FDR $< 0.05$ in each relevant comparison. GSEA preranked analysis of signaling pathways from the Oncogenic signature gene sets was performed using the Java version of the software (gsea2–2.2.3.jar; software.broadinstitute.org/gsea/), with log2FC obtained from RNA-Seq contrasts and standard parameters.

## Endothelial tube formation assay

HUVEC were seeded at a concentration of $3 \times 10^4$ cells in a 96-well culture plate pre-coated with Cultrex® Basement Membrane Extract (Trevigen, MD, U.S.A., 50 µl/well) and stimulated with serum-free medium with ET-1, CM derived from PD-HG-SOC cells and WI-30 previously treated with macitentan or bevacizumab, alone or in combination. After 24 h, illustrative images of tube formations were captured in the ZOE Fluorescent Cell Image (20× magnification; Bio-Rad).

## Collagen gel contraction assay

Collagen gel was prepared according to the manufacturer's protocol (Corning, Bedford, MA, U.S.A.). Collagen solution was neutralized by adding 12 µl of Ac. Acetic 0.1% and 7µl of 1 M NaOH to 600 µl of Type-I collagen stock solution (3 mg/ml). Then, WI-38 fibroblasts ($1.5 \times 10^3$) suspended in 500 µl of cell culture media were added and gently mixed. The cell-laden collagen was transferred into 24-well plates and incubated at 37°C for 30 min. Collagen polymerized forming disk-shaped gels were gently detached from the edges of the culture wells. Following, the disk-shaped gels were stimulated with ET-1 and/or treated with macitentan or bevacizumab and incubated at 37°C and 5% $CO_2$ for 24 h and then photographed. The decrease of the surface area ($cm^2$) of the disk-shaped gels was used to quantify the degree of gel contractility that was measured by ImageJ program.

## Hybrid HG-SOC/fibroblast 3D spheroid sprouting assay

A three-dimensional sprouting assay with hybrid spheroids composed by PD-HG-SOC cells/fibroblasts, obtained by plating 100 cells per well in 3D Culture Qualified 96-well plates. After 48 h, spheroids were embedded into the Cultrex matrix and treatments were made. Spheroids were photographed at time 0 and after the treatments using a ZOE Fluorescent Cell Imager (Bio-Rad) and their sprout length was quantified using ImageJ program.

## Migration and invasion assays

The cell migratory and invasive ability was determined using transwell migration and matrigel invasion assays, by using a Boyden chambers (BD Biosciences, NJ, U.S.A.) and a Matrigel Invasion Chamber (BD Biosciences), respectively. In brief, PD HG-SOC cells ($5 \times 10^4$) were seeded in the upper part of chambers and stimulated in the lower part of chambers with serum-free medium alone, or in the presence of ET-1, or upon the addition of macitentan or bevacizumab. After 48 h, the migrating and invading cells were visualized using a Diff-Quick kit (Dade Behring, IL, U.S.A.) and detected under a ZOE Fluorescent Cell Imager (Bio-Rad). Migrating and invading cells were counted using the ImageJ program.

## Statistical analysis

Student's *t*-test was used for the analysis of the comparison between two groups of independent samples. Data points represent the mean and standard deviation (SD) of three independent experiments performed in triplicates for all the conditions described. The analysis of the data was conducted in GraphPad Prism v8.0 software.

# Results

## The ET-1/ET-1R FFL intertwines with the VEGF/VEGFR axis and sustains pro-survival signals in HG-SOC and stromal cells

To identify ligand/receptor pairs that in response to ET-1 signaling activation could exert an active role in the heterotypic tumor/TME networking, we performed a RNAseq analysis in PD-HG-SOC cells. The HG-SOC transcriptional analysis recognized *VEGFA* pathway among the mostly up-regulated in response to ET-1 and down-regulated

*Clinical Science* (2024) **138** 851–862
https://doi.org/10.1042/CS20240346

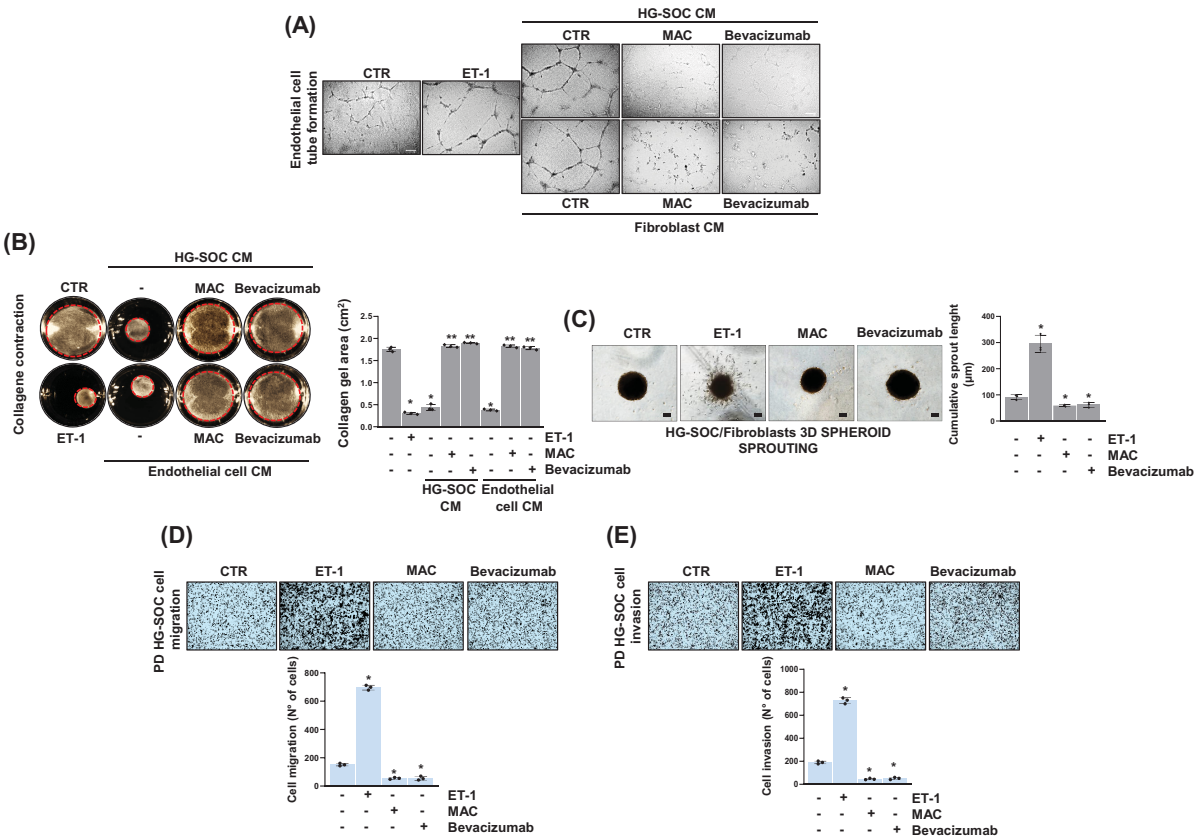


**Figure 3. Macitentan, blocking the ET-1/ET-1R and VEGF/VEGFR FFL, prevents HG-SOC invasion**

(**A**) Tube formation assay of endothelial cells (EC) stimulated or not with ET-1 or exposed to the conditioned media (CM) derived by PD-HG-SOC cells or fibroblasts pre-treated or not with MAC or bevacizumab. Representative images of the tubes were photographed (scale bar: 100 μm, magnification 20×; $n$=3). (**B**) Collagen contraction assay of activated fibroblasts stimulated or not with ET-1 or exposed to the CM derived by PD-HG-SOC cells or EC pre-treated or not with MAC or bevacizumab. Images of the collagen contraction assay are representative of three independently performed experiments (left panels). The right graph indicates the collagen gel area. Bars are means ± SD (*$P$<0.0002 vs. not stimulated fibroblasts; **$P$<0.0002 vs. activated fibroblasts stimulated with CM derived from PD-HG-SOC cells or EC not pre-treated with MAC or bevacizumab; $n$=3). (**C**) Representative images of 3D hybrid PD-HG-SOC/activated fibroblasts spheroids sprouting into the surrounding matrix upon stimulation with exogenous ET-1 or upon treatment with MAC or bevacizumab for 48 h (scale bar: 100 μm, magnification 10×). *Right graph*, quantification of cumulative sprout length (μM). Bars are means ± SD (*$P$<0.03 vs. untreated spheroids; $n$=3). (**D,E**) Migration and invasion assays of PD HG-SOC cells stimulated or not with ET-1, or treated with MAC or bevacizumab for 48 h. Representative images of migratory and invading cells were photographed (scale bar: 100 μm, magnification: 20×) (upper panels) or counted (bottom graphs). Bars are means ± SD (*$P$<0.0006 vs. CTR; $n$=3).

upon treatment with macitentan (Figure 1A and Supplementary Table S1). Remarkably, gene set enrichment analysis (GSEA) identified a strong signal in the VEGFA signature, emphasizing the ability of the ET-1 signaling to regulate the VEGF-related angiogenic processes (Figure 1B). Along with these results, we detected how not only PD-HG-SOC cells but also stromal components as the endothelial cells (EC) and activated fibroblasts, expressed VEGF and its cognate receptors VEGFR1 and VEGFR2, as well as ET-1 and the $ET_AR$ and $ET_BR$ (Figure 1C). This observation paves the way to the intriguing perspective that the VEGF/VEGFR and ET-1/ET-1R axes, in response to ET-1 signaling initiation, could be actively implicated in the tumor/TME cross-talk. In both tumor and stromal cells, ET-1 up-regulated the expression of HIF-1α and VEGF, an effect hindered by the ET-1R targeting with macitentan. Of interest, VEGF increased both HIF-1α and ET-1 expression, that were down-modulated by the anti-VEGF antibody bevacizumab (Figure 1D,E), highlighting the inter-regulation existing between these two signaling pathways.

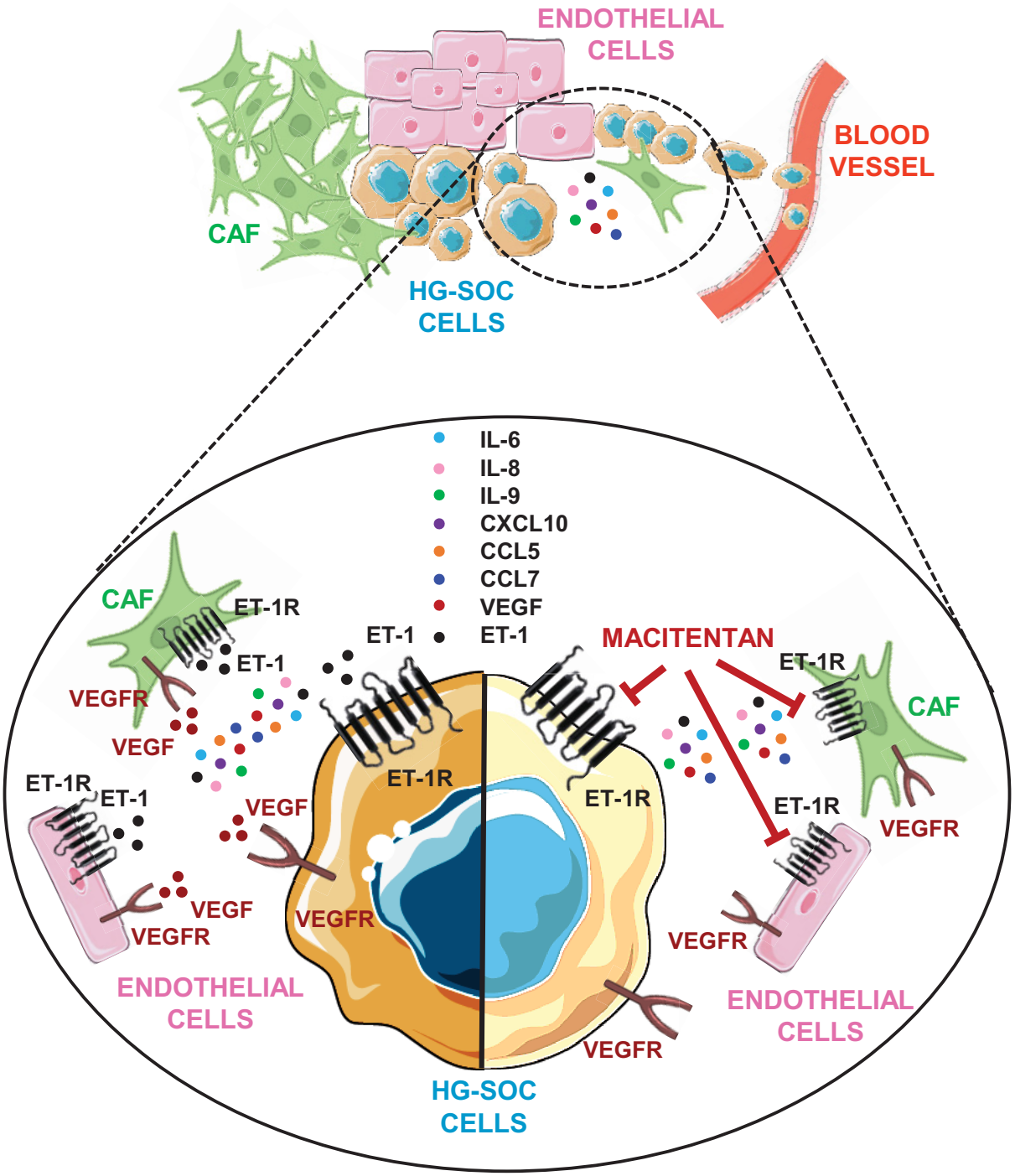


**Figure 4. Graphic model depicting the role of the ET-1/ET-1R and VEGF/VEGFR FFL at the root of the HG-SOC/TME communication**

The ET-1/ET-1R axis, directing the activation of the interweaved ET-1/ET-1R and VEGF/VEGFR FFL, concurrently in PD-HG-SOC cells, endothelila cells (EC) and activated fibroblasts, fine-tunes the tumoral and stromal cell secretome toward a pro-tumoral configuration and reawakens the neighboring TME cells to establish a tumor supportive niche, empowering HG-SOC progression. Of clinical impact, macitentan, shutting down the ET-1/ET-1R-driven signals, halts the HG-SOC invasive and metastatic potential. This knowledge emphasizes how a more effective treatment schedule for HG-SOC should be centred on the use of tumor/TME simultaneously targeting therapeutics, as the dual ET-1R antagonist macitentan able to turn off the aberrantly activated signals in the HG-SOC cells but also in the TME. Part of the figure is drawn using pictures from Servier Medical Art (https://smart.servier.com), licensed under a Creative Commons Attribution 3.0 Unported License (https://creativecommons.org/licenses/by/3.0).

*Clinical Science* (2024) **138** 851–862
https://doi.org/10.1042/CS20240346

Moving toward this framework, we observed that cell stimulation with ET-1 and VEGF, concurrently in PD-HG-SOC cells, EC and activated fibroblasts, sustained the induction of pro-survival signals, as shown by the ET-1- and VEGF-triggered activation of p42/44 MAPK and AKT, which was abrogated upon treatment with macitentan or bevacizumab (Figure 1F). Overall, the present results demonstrate how the ET-1/ET-1R and VEGF/VEGFR FFL represent a HG-SOC/TME inter-regulatory shared signaling to reciprocally communicate.

## The ET-1/ET-1R FFL shapes the tumor and TME secretome pattern

Given the regulatory role exercised by the tumoral and stromal secretome in transmitting messages that impact on the metastatic attitude [3,9], we characterized the PD-HG-SOC cell, EC and activated fibroblast CM composition in response to ET-1. This analysis revealed that ET-1 stimulation improved the release of a subset of pro-inflammatory interleukins, as IL-1β, IL-2, IL-6, IL-8 and IL-9, chemokines, as CCL5 and CCL7, and growth factors, including VEGF, M-CSF, MIF, SCGF-β in PD-HG-SOC cells, EC and activated fibroblasts, whose release was diminished upon treatment with macitentan (Figure 2A–C). Remarkably, IL-6, IL-8, IL-9, CXCL10, CCL5, CCL7 and VEGF were the molecules commonly released by PD-HG-SOC cells, EC and fibroblasts (Figure 2D).

To validate these results, we measured the ET-1 and VEGF release by ELISA, further proving that all the cells released both ET-1 and VEGF (Figure 2E,F) at a basal level of approximately 200 pg/ml and 300 pg/ml per $1 \times 10^6$ cells, respectively, and that VEGF secretion was boosted upon cell stimulation with ET-1 (Figure 2F). The physical interaction of PD-HG-SOC cells with EC or activated fibroblasts in double co-cultures enhanced the secretion of both ET-1 and VEGF, compared with the single cell culture. This effect was more marked in the triple PD-HG-SOC/EC/fibroblasts co-culture systems. Macitentan, mimicking the effect of bevacizumab, interfered with ET-1 and VEGF release (Figure 2E,F). These results emphasize the significance of the interplay existing between tumor cells and stromal components in HG-SOC and how, in the intricate network of HG-SOC/TME-released soluble mediators ET-1 and VEGF activate self-sustaining signaling flows that are blocked by ET-1R targeting drugs.

## The administration of macitentan, preventing the HG-SOC/TME shared ET-1/ET-1R FFL, hinders the HG-SOC invasive behavior

To examine whether in response to the ET-1/ET-1R FFL, the HG-SOC cells, EC and activated fibroblasts undergo functional changes that contribute to enforce the HG-SOC invasive behavior, we performed a set of functional assays. In particular, we observed that the ET-1/ET-1R FFL improved the EC angiogenic ability. The tube formation assay unveiled that ET-1 addition to EC, similarly to EC stimulation with PD-HG-SOC- or fibroblast-derived CM boosted their ability to form vascular-like structures. Conversely, EC stimulation with CM derived from PD-HG-SOC or fibroblasts pre-treated with macitentan, or bevacizuman precluded such ability (Figure 3A).

To validate the prominent role of the ET-1-guided FFL in fostering the HG-SOC metastatic dissemination route, and considering how the activation of fibroblasts, intensively involved in extracellular matrix (ECM) deposition and remodelling, bolsters tumor progression and metastases, we examined the collagen-contraction ability of fibroblasts in response to the ET-1 stimulation. In particular, we observed that fibroblasts stimulated with ET-1 were characterized by the ability to contract collagen, the main ECM component (Figure 3B). Of note, the effect produced by fibroblast stimulated with ET-1 was comparable to that one produced by fibroblast stimulation with CM derived from PD-HG-SOC cells or EC. In contrast, the inhibition of the ET-1/ET-1R FFL upon treatment with macitentan, similarly to bevacizumab, impaired collagen contraction (Figure 3B), clearly proving the involvement of the two ligand-receptor pair-driven signaling in supporting the unfavorable fibroblast behavior, which represents a hallmark of an invasive and metastatic HG-SOC [16]. Furthermore, we set-up a 3D experimental system to test the PD HG-SOC metastatic behavior, represented by hybrid spheroids incorporating PD-HG-SOC and fibroblasts, in quality of stromal element, embedded into a biomimetic matrix, mimicking the HG-SOC ECM, observing that stimulation with ET-1 sustained the formation of invasive sprouts of a greater length compared with untreated spheroids. The ET-1-potentiated spheroid ability to invade the surrounding matrix was prevented upon ET-1/ET-1R FFL blockade by macitentan, to an extent similar to that one observed in presence of bevacizumab (Figure 3C). To strength the major role of the ET-1-driven FFL in fuelling the HG-SOC aggressive traits, we extended this analysis by examining the PD HG-SOC cell migratory and invasive pattern, confirming that cell stimulation with ET-1 boosted the HG-SOC migratory and invasive potential, an effect hindered by macitentan, as well as upon cell treatment with bevacizumab (Figure 3D,E). Collectively, these findings suggest that the activation of the ET-1/ET-1R-mediated FFL simultaneously in tumor cells and stromal components, which live and expand nearby tumor cells, sustains the HG-SOC metastatic course.

## Discussion

In the intricate HG-SOC ecosystem, the identification of the heterotypic connection existing within the TME offers, on one side, the prospective to impact on disease initiation and progression, and, on the other, to design therapies to tackle the tumor and normalize the TME, in an effort to improve patient life expectancy. In such dangerous tumor/TME affair the cell secretome, that include potent and multifaceted released modulators, as cytokines, chemokines and growth factors, play a leading role. Recent evidences demonstrated that such circulating molecules, activating vicious FFL at the tumor/TME interface, transmit reprogramming signals to both cancer and stromal cells that prime and establish a tumor supportive niche [9], thus highlighting how these FFL are worthy of investigation to refine new therapeutic strategies.

In the present study, using double and triple co-culture systems, we identified two co-regulated FFL, the ET-1/ET-1R and VEGF/VEGFR ligand/receptor pairs, concurrently activated by ET-1 in PD-HG-SOC cells, EC and activated fibroblasts. The intertwined regulated FFL-driven pro-survival signals adjust the tumoral and stromal secretome toward a pro-tumoral configuration, renew the EC and the activated fibroblast dangerous behavior and enforce the HG-SOC invasive attitude. From a clinical perspective, ET-1R blockade by macitentan, impairing the FFL-driven HG-SOC/TME reciprocal signaling network, interfered with the HG-SOC invasive strength (Figure 4).

These observations are aligned with previous findings demonstrating how in HG-SOC the ET-1 elicits pleiotropic effects simultaneously on tumor cells and the host microenvironment, representing a life raft to survive to anticancer drugs [24], including the PARPi olaparib [16]. Along with these observations, recent reports highlight the potentiality of ET-1R antagonists to abrogate the tumor-supportive features of several components of the TME, including macrophages, fibroblasts and immune cells, suppressing tumor growth [25,26], and potentiating the efficacy of antimetastatic drugs, as the immune checkpoint inhibitors (ICI) [27].

For the HG-SOC patient clinical management one of the most promising therapeutic approaches, approved for the first-line maintenance treatment, is based on the use of angiogenesis targeting agents, as bevacizumab [28–30]. Related to this aspect, it was reported how this antibody, normalizing the TME, may improve the efficacy of various anticancer treatments [31,32]. Interestingly, anti-angiogenesis therapy, including ET-1R and VEGF blockade, represent one of the tools available to restore T-cell infiltration in HG-SOC and could be implemented in combination therapy with ICI [33]. In line with these studies, our results expand the multi-faceted function of ET-1 in orchestrating the tumor/stroma communication supporting the potential role of ET-1R antagonists in effective combination therapy.

In order to recreate a valuable tool that allow an in-depth understanding of the cancer–host interaction that take place within the tumor, our future studies will head toward the setting and optimization of PD organotypic experimental models incorporating PD HG-SOC paired tumor cells, generated from primary solid tumors and after recurrence, along with PD TME elements and biomimetic matrices. These models, mirroring the HG-SOC patient features, may be used to refine personalized treatments.

Overall, the present study supports the concept that to accomplish long-term successful therapies, the anticancer drugs should hit the communication between tumor cells and the surrounding TME elements. In this perspective macitentan, as a dual ET-1R antagonist, holds the power to interfere at once with $ET_AR$ expressed on tumor cells and to prevent the support to the tumor provided by the TME elements, mostly expressing $ET_BR$, hindering the HG-SOC/TME features related to malignant progression. Our preclinical findings, identifying the intertwined ET-1 and VEGF FFL as two HG-SOC/TME shared vulnerabilities, may provide a clinical guideline to expand and refine the repertoire of treatment strategies in HG-SOC patients with a marked up-regulation of the ET-1 system. Therefore, targeting the ET-1R may emerge as an effective therapy for metastasis as it can simultaneously target the HG-SOC cells and potentially normalize the TME.

### Clinical perspectives

- In recent years, the HG-SOC TME has been described to heavily bolster tumor progression and therapy elusion. However, a wide-ranging view of the tumor/TME communication strategies instructed by the ET-1-driven signaling deserve to be further investigated.
- This research corroborates how at the HG-SOC/TME interface the ET-1/ET-1R and VEGF/VEGFR FFL contribute to fine-tune simultaneously the tumoral and stromal cell secretome toward a pro-invasive pattern, empowering the TME cell pro-invasive behavior and strengthening HG-SOC progression.

*Clinical Science* (2024) **138** 851–862
https://doi.org/10.1042/CS20240346

- From a clinical outlook, the recognition of ET-1R-driven co-regulated FFL as intermediaries of the HG-SOC/TME communication, lay the basis for targeting ET-1R to hinder the tumor/TME communication route.

## Data Availability

The Data Availability Statement was included in the main manuscript file, as reported below: "All data generated and analysed during the current study are included in this article or from the corresponding authors (A.B. or P.T.) on reasonable request. The raw data are included as supplementary materials. PD-HG-SOC cells will be made available to academic researchers with material transfer agreement. All data and reagents are available from the authors upon request. GSEA: Public available data used in this article were obtained from: GSEA Gene Set Enrichment Analysis (https://www.gsea-msigdb.org/gsea/index.jsp). The RNA-seq data have been deposited at the GEO repository database with the accession code GSE268498."

## Competing Interests

The authors declare that there are no competing interests associated with the manuscript.

## Funding

The research leading to these results was supported by Fondazione AIRC [grant number AIRC IG22835]; Ministero della Salute [grant number RF-2019-12368718]; MUR-PNRR M4C2I1.3 PE6 project PE00000019 Heal Italia [grant number CUP H83C22000550006 (to A.B. and G.B.)]; and by Fondazione AIRC [grant number MFAG 2023 ID. 28919 (to P.T.)].

## CRediT Author Contribution

**Piera Tocci:** Conceptualization, Data curation, Formal analysis, Funding acquisition, Investigation, Methodology, Writing—original draft. **Celia Roman:** Data curation, Investigation, Methodology. **Rosanna Sestito:** Data curation, Investigation, Methodology. **Valentina Caprara:** Data curation, Investigation, Methodology. **Andrea Sacconi:** Data curation, Software, Investigation. **Ivan Molineris:** Data curation, Formal analysis, Methodology. **Giovanni Tonon:** Data curation, Formal analysis, Supervision. **Giovanni Blandino:** Supervision, Writing—review & editing. **Anna Bagnato:** Conceptualization, Data curation, Supervision, Funding acquisition, Project administration, Writing—review & editing.

## Ethics Approval

Ascitic fluids samples were obtained with the written consent of HG-SOC patients undergoing surgery for ovarian tumor at the Gynecological Oncology of IRCCS, Regina Elena National Cancer Institute of Rome. The study protocol for ascites collection and clinical information was approved by the Regina Elena Cancer Institute review board (IRB). All protocols involving human specimens are compliant with all relevant ethical regulations.

## Code Availability

The RNA-seq data have been deposited at the GEO repository database with the accession code GSE268498.

## Acknowledgements

We gratefully acknowledge Maria Vincenza Sarcone for administrative support. The research leading to these results was supported by Fondazione AIRC (AIRC IG22835), Ministero della Salute (RF-2019-12368718) and MUR-PNRR M4C2I1.3 PE6 project PE00000019 Heal Italia (CUP H83C22000550006) to A.B. and by Fondazione AIRC (MFAG 2023 ID. 28919) to P.T.

## Abbreviations

AIRC, Italian Foundation for Cancer Research; CM, Conditioned Media; CPM, Counts Per Million; EC, Endothelial Cell; ECL, Enhanced Chemiluminescence; ECM, Extracellular Matrix; ET-1, Endothelin-1; ET-1R, Endothelin-1 receptor; $ET_AR$, Endothelin-1 A receptor; $ET_BR$, Endothelin-1 B receptor; FFL, Feed-forward loops; GLM, Generalized Linear Model; GSEA, Gene Set Enrichment Analysis; HG-SOC, High-Grade Serous Ovarian Cancer; HIF-1$\alpha$, Hypoxia Inducible Factor-1$\alpha$; IB, Immunoblotting; ICI, Immune checkpoint inhibitors; IRB, Regina Elena Institutional Review Board; LF, Likelihood F; PD, Patient-derived; RIN, RNA Integrity Number; RPKM, Reads Per Kilobase Million; SD, Standard Deviation; TME, Tumor microenvironment; TMM, Trimmed-mean of M-values; VEGF, Vascular endothelial growth factor; VEGFR1, Vascular endothelial growth factor 1; VEGFR2, Vascular endothelial growth factor 2.

## References

1 Bhat, B.A., Saifi, I., Khamjan, N.A., Hamdani, S.S., Algaissi, A., Rashid, S. et al. (2023) Exploring the tumor immune microenvironment in ovarian cancer: a way-out to the therapeutic roadmap. *Expert Opin. Ther. Targets* **27**, 841–860, https://doi.org/10.1080/14728222.2023.2259096
2 de Visser, K.E. and Joyce, J.A. (2023) The evolving tumor microenvironment: From cancer initiation to metastatic outgrowth. *Cancer Cell* **41**, 374–403, https://doi.org/10.1016/j.ccell.2023.02.016
3 Tang, P.W., Frisbie, L., Hempel, N. and Coffman, L. (2023) Insights into the tumor-stromal-immune cell metabolism cross talk in ovarian cancer. *Am. J. Physiol. Cell Physiol.* **325**, C731–C749, https://doi.org/10.1152/ajpcell.00588.2022
4 Kim, S., Kim, B. and Song, Y.S. (2016) Ascites modulates cancer cell behavior, contributing to tumor heterogeneity in ovarian cancer. *Cancer Sci.* **107**, 1173–1178, https://doi.org/10.1111/cas.12987
5 Ferri-Borgogno, S., Zhu, Y., Sheng, J., Burks, J.K., Gomez, J.A., Wong, K.K. et al. (2023) Spatial transcriptomics depict ligand-receptor cross-talk heterogeneity at the tumor-stroma interface in long-term ovarian cancer survivors. *Cancer Res.* **83**, 1503–1516, https://doi.org/10.1158/0008-5472.CAN-22-1821
6 Pearce, O.M.T., Delaine-Smith, R.M., Maniati, E., Nichols, S., Wang, J., Böhm, S. et al. (2018) Deconstruction of a metastatic tumor microenvironment reveals a common matrix response in human cancers. *Cancer Discov.* **8**, 304–319, https://doi.org/10.1158/2159-8290.CD-17-0284
7 Lan, C., Heindl, A., Huang, X., Xi, S., Banerjee, S., Liu, J. et al. (2015) Quantitative histology analysis of the ovarian tumour microenvironment. *Sci. Rep.* **5**, 16317, https://doi.org/10.1038/srep16317
8 Heindl, A., Lan, C., Rodrigues, D.N., Koelble, K. and Yuan, Y. (2016) Similarity and diversity of the tumor microenvironment in multiple metastases: critical implications for overall and progression-free survival of high-grade serous ovarian cancer. *Oncotarget* **7**, 71123–71135, https://doi.org/10.18632/oncotarget.12106
9 Baumann, Z., Auf der Maur, P. and Bentires-Alj, M. (2022) Feed-forward loops between metastatic cancer cells and their microenvironment-the stage of escalation. *EMBO Mol. Med.* **8**, e14283, https://doi.org/10.15252/emmm.202114283
10 Labiche, A., Heutte, N., Herlin, P., Chasle, J., Gauduchon, P. and Elie, N. (2010) Stromal compartment as a survival prognostic factor in advanced ovarian carcinoma. *Int. J. Gynecol. Cancer* **20**, 28–33, https://doi.org/10.1111/IGC.0b013e3181bda1cb
11 Stur, E., Corvigno, S., Xu, M., Chen, K., Tan, Y., Lee, S. et al. (2022) Spatially resolved transcriptomics of high-grade serous ovarian carcinoma. *iScience* **25**, 103923, https://doi.org/10.1016/j.isci.2022.103923
12 Launonen, I.M., Lyytikäinen, N., Casado, J. et al. (2022) Single-cell tumor-immune microenvironment of BRCA1/2 mutated high-grade serous ovarian cancer. *Nat. Commun.* **13**, 835, https://doi.org/10.1038/s41467-022-28389-3
13 Tocci, P., Rosanò, L. and Bagnato, A. (2019) Targeting endothelin-1 receptor/β-arrestin-1 axis in ovarian cancer: from basic research to a therapeutic approach. *Front. Endocrinol. (Lausanne)* **10**, 609, https://doi.org/10.3389/fendo.2019.00609
14 Tocci, P., Cianfrocca, R., Di Castro, V., Rosanò, L., Sacconi, A., Donzelli, S. et al. (2019) β-arrestin1/YAP/mutant p53 complexes orchestrate the endothelin A receptor signaling in high-grade serous ovarian cancer. *Nat. Commun.* **10**, 3196, https://doi.org/10.1038/s41467-019-11045-8
15 Tocci, P., Cianfrocca, R., Sestito, R., Rosanò, L., Di Castro, V., Blandino, G. et al. (2020) Endothelin-1 axis fosters YAP-induced chemotherapy escape in ovarian cancer. *Cancer Lett.* **492**, 84–95, https://doi.org/10.1016/j.canlet.2020.08.026
16 Tocci, P., Roman, C., Sestito, R., Di Castro, V., Sacconi, A., Molineris, I. et al. (2023) Targeting tumor-stroma communication by blocking endothelin-1 receptors sensitizes high-grade serous ovarian cancer to PARP inhibition. *Cell Death Dis.* **14**, 5, https://doi.org/10.1038/s41419-022-05538-6
17 Bekes, I., Friedl, T.W.P., Köhler, T., Möbus, V., Janni, W., Wöckel, A. et al. (2016) Does VEGF facilitate local tumor growth and spread into the abdominal cavity by suppressing endothelial cell adhesion, thus increasing vascular peritoneal permeability followed by ascites production in ovarian cancer? *Mol. Cancer* **15**, 13, https://doi.org/10.1186/s12943-016-0497-3
18 Horikawa, N., Abiko, K., Matsumura, N., Hamanishi, J., Baba, T., Yamaguchi, K. et al. (2017) Expression of vascular endothelial growth factor in ovarian cancer inhibits tumor immunity through the accumulation of myeloid-derived suppressor cells. *Clin. Cancer* **23**, 587–599, https://doi.org/10.1158/1078-0432.CCR-16-0387
19 Salani, D., Di Castro, V., Nicotra, M.R., Rosanò, L., Tecce, R., Venuti, A. et al. (2000) Role of endothelin-1 in neovascularization of ovarian carcinoma. *Am. J. Pathol.* **157**, 1537–1547, https://doi.org/10.1016/S0002-9440(10)64791-8
20 Rosanò, L., Spinella, F. and Bagnato, A. (2013) Endothelin 1 in cancer: biological implications and therapeutic opportunities. *Nat. Rev. Cancer* **13**, 637–651, https://doi.org/10.1038/nrc3546
21 Dobin, A., Davis, C.A., Schlesinger, F., Drenkow, J., Zaleski, C., Jha, S. et al. (2013) STAR: ultrafastuniversal RNA-seqaligner. *Bioinformatics* **29**, 15–21, https://doi.org/10.1093/bioinformatics/bts635
22 Liao, Y., Smyth, G.K. and Shi, W. (2014) Feature Counts: an efficient general purpose program for assigning sequence reads to genomic features. *Bioinformatics* **9**, 23–30
23 Robinson, M.D., McCarthy, D.J. and Smyth, G.K. (2010) edgeR: a bioconductor package for differential expression analysis of digital gene expression data. *Bioinformatics* **26**, 139–140, https://doi.org/10.1093/bioinformatics/btp616
24 Rosanò, L., Cianfrocca, R., Tocci, P., Spinella, F., Di Castro, V., Caprara, V. et al. (2014) Endothelin A receptor/β-arrestin signaling to the Wnt pathway renders ovarian cancer cells resistant to chemotherapy. *Cancer Res.* **74**, 7453–7464, https://doi.org/10.1158/0008-5472.CAN-13-3133
25 Weigert, A., Zheng, X., Nenzel, A., Turkowski, K., Günther, S., Strack, E. et al. (2022) Fibrocytes boost tumor-supportive phenotypic switches in the lung cancer niche via the endothelin system. *Nat. Commun.* **13**, 6078, https://doi.org/10.1038/s41467-022-33458-8
26 Arndt, P.F., Turkowski, K., Cekay, M.J., Eul, B., Grimminger, F. and Savai, R. (2024) Endothelin and the tumor microenvironment: a finger in every pie. *Clin. Sci. (Lond.)* **138**, 617–634, https://doi.org/10.1042/CS20240426
27 Son, S., Shin, J.M., Shin, S., Kim, C.H., Lee, J.A., Ko, H. et al. (2021) Repurposing macitentan with nanoparticle modulates tumor microenvironment to potentiate immune checkpoint blockade. *Biomaterials* **276**, 121058, https://doi.org/10.1016/j.biomaterials.2021.121058

*Clinical Science* (2024) **138** 851–862
https://doi.org/10.1042/CS20240346

28 Ray-Coquard, I., Pautier, P., Pignata, S., Pérol, D., González-Martín, A., Berger, R. et al. (2019) Olaparib plus bevacizumab as first-line maintenance in ovarian cancer. *N. Engl. J. Med.* **381**, 2416–2428, https://doi.org/10.1056/NEJMoa1911361
29 Mao, C.L., Seow, K.M. and Chen, K.H. (2022) The utilization of bevacizumab in patients with advanced ovarian cancer: a systematic review of the mechanisms and effects. *Int. J. Mol. Sci.* **23**, 6911, https://doi.org/10.3390/ijms23136911
30 Lorusso, D., Mouret-Reynier, M.A., Harter, P., Cropet, C., Caballero, C., Wolfrum-Ristau, P. et al. (2023) Updated progression-free survival and final overall survival with maintenance olaparib plus bevacizumab according to clinical risk in patients with newly diagnosed advanced ovarian cancer in the phase III PAOLA-1/ENGOT-ov25 trial. *Int. J. Gynecol. Cancer* **21**, 550–558, https://doi.org/10.1136/ijgc-2023-004995
31 Mpekris, F., Voutouri, C., Baish, J.W., Duda, D.G., Munn, L.L., Stylianopoulos, T. et al. (2020) Combining microenvironment normalization strategies to improve cancer immunotherapy. *Proc. Natl. Acad. Sci. U.S.A.* **117**, 3728–3737, https://doi.org/10.1073/pnas.1919764117
32 Pilié, P.G., Tang, C., Mills, G.B. and Yap, T.A. (2019) State-of-the-art strategies for targeting the DNA damage response in cancer. *Nat. Rev. Clin. Oncol.* **16**, 81–104, https://doi.org/10.1038/s41571-018-0114-z
33 Kandalaft, L.E., Dangaj Laniti, D. and Coukos, G. (2022) Immunobiology of high-grade serous ovarian cancer: lessons for clinical translation. *Nat. Rev. Cancer* **22**, 640–656, https://doi.org/10.1038/s41568-022-00503-z